Accurate Detection of 3D Tubular Tree Structures

Nicolas Flasque, Michel Desvignes, Jean-Marc Constans, Marinette Revenu

Accurate Detection of 3D Tubular Tree Structures

Nicolas Flasque[(1)], Michel Desvignes[(1)], Jean-Marc Constans[(2)], Marinette Revenu[(1)]

(1) Greyc Image ISMRA – CNRS UMR 6072 – 6, Bd du Maréchal Juin F-14050 CAEN Cedex
(2) Service d'IRM du CHU de CAEN – Avenue de la Côte de Nacre F-14000 CAEN

ABSTRACT

Spatial resolution of Magnetic Resonance Angiography (MRA) makes it a powerful tool for diagnosis and surgical planning. However, image interpretation and visualization tools are missing, and three-dimensional measurements are not usually accessible [6]. Flexible visualization of the whole vascular tree and precise quantification of phenomenons like carotid stenosis are applications of an automated processing of MRA [5]. Building an accurate model of a tubular objects network such as bronchi or blood vessels can provide a substantial help for 3D visualization and quantification [4].

We present the tracking algorithm of centrelines that makes very few assumptions on the structure grey-level profile. The main originality of this work is the accurate 3D centreline tracking process which provides subvoxel accuracy and deals with bifurcations. This approach has been successfully applied to the cerebral vasculature in MRA images.

1. INTRODUCTION

Medical imaging modalities such as Magnetic Resonance or Scanner are able to provide high-quality 3D images of various body areas. Extracting and processing 3D structures from those images is an important issue, as visualization and quantification problems are much more difficult than for 2D modalities.

Many different approaches exist to address this issue : linear multiscale analysis with a structure model, grey-level model matching, skeletonization, iterative methods, detection of structures using filters, and curve or surface optimisation.

Once one of these methods is used, one can obtain a set of primitives : 2D or 3D analytically defined centrelines,voxels or points ordered lists, connected or disconnected linear segments, regions, probability maps, sets of regions of interest, or edges.

Not all of these methods and extracted primitives are suited for an accurate representation of structures.

We present an iterative tracking method that detects the centreline of a 3D tubular structure with subvoxel accuracy and that is suited for further visualization and quantification issues.

2. METHOD

2.1. Tubular structure extraction

A segmentation step applied to original images provides unstructured sets of connected voxels. The structures of interest have to be identified from those sets. We use a two-step approach to extract tubular tree structures from the 3D image : centerline tracking with detection of bifurcation and tree representation of the network.

2.2. Centerline tracking

Tracking is an iterative process with subvoxel accuracy. It detects the centerline of tubular objects using the segmented image. To insure subvoxel accuracy, tracking has to be processed in a continuous 3D space obtained by interpolation. A set of centreline points $\{P_i\}$ is computed by this method and interpolated by a B-spline curve [1].

From a point given point P_i and a given direction D_i, a local computation is done in a search area to find the point P_{i+1} and direction D_{i+1}. The search area is a mobile parallelepiped built (Fig. 1) at each step according to P_i and D_i values. The dimensions of the parallelepiped, L_i, l_i and H_i are computed dynamically and evolve with estimated object diameter and local curvature.

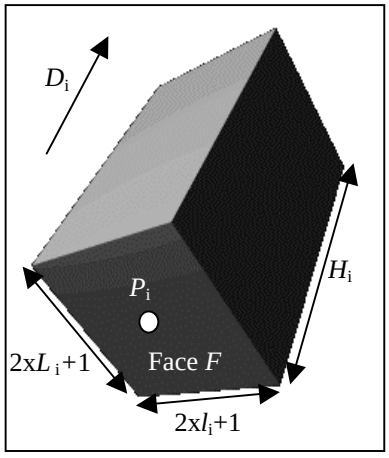

Figure 1 : the local search area with parameters $\{P_i, D_i, L_i, l_i, H_i\}$

Let P_i be the current point and D_i the current tracking direction.

Let L_i, l_i and H_i be the dimensions of the box in integer number of voxel.

Let $\alpha \in [-l_i ; l_i]$, $\beta \in [-L_i ; L_i]$, $\gamma \in [0, H_i]$.

Let $X_{\alpha,\beta,\gamma} = P_i + \begin{pmatrix} \alpha \\ \beta \\ \gamma \end{pmatrix} \overrightarrow{D_i}$,

and $A_{\alpha,\beta,\gamma}$ a weight associated to $X_{\alpha,\beta,\gamma}$.

The interpolated intensity at $X_{\alpha,\beta,\gamma}$ is noted $Im(\alpha,\beta,\gamma)$.

$$B_i = \frac{1}{Card(V)} \times \frac{\sum_{X\alpha,\beta,\gamma} A_{\alpha,\beta,\gamma} \times X_{\alpha,\beta,\gamma}}{\sum_{X\alpha,\beta,\gamma} A_{\alpha,\beta,\gamma}}$$

$$V = \left\{ X_{\alpha,\beta,\gamma} / A_{\alpha,\beta,\gamma} > 0 \right\}$$

$$P_{i+1} = \frac{(k_p . P_i) + B_i}{k_p + 1}$$

$$\overrightarrow{D_{i+1}} = \frac{\dfrac{\overrightarrow{D_i}}{\left\| \overrightarrow{D_i} \right\|} + k_d . \left(\dfrac{\overrightarrow{B_i - P_i}}{\left\| \overrightarrow{B_i - P_i} \right\|} \right)}{k_d + 1}$$

Parameters k_p and k_d have a fixed value corresponding to the maximal curvature of vessels that can be tracked by this technique. For a given set $\{k_p, k_d\}$, the maximum curvature that can be estimated by the tracking algorithm is limited by the dimensions of the paralleliped which are computed at each step of the tracking.

2.3. Detection of bifurcations

In order to detect bifurcations and end of structures, connnectivity informations are used. Two quantities are computed : NV, the number of volumic connected components inside the parallelepiped, and NS, the number of surfacic connected components at the boundaries of the parallelepiped. Relative values of these quantities indicate whether to check for a bifurcation (Fig. 2b) or not (Fig. 2a). Values of NV and NS both equal to 1 indicate an end of structure.

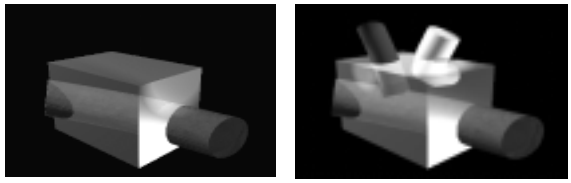

a) NV = 1; NS = 2 b) NV = 2; NS = 5

Figure 2 : Possible voxel configurations inside the parallelepiped with NV and NS values.

3. ACCURACY OF THE METHOD

Several different synthetic image sets have been used to test the various aspects of the tracking algorithm (Fig. 3) : straight tubes, 3 3D-Lissajoux shapes, and Y-fork shapes with angle varying from 20° to 160° by a step of 20°. All images are generated using a second-order B-spline curve. The orthogonal plane is calculated along the spline course and the cross section is generated in each plane. For each shape, 4 diameters are generated :1, 2, 4 and 6 voxels. The intensity profile of the generated section is a gaussian.

Difference in position between the nearest points (ΔP) and difference in orientation between those points ($\Delta\Theta$) are measured between the synthetic object centerline and the detected B-spline curve.

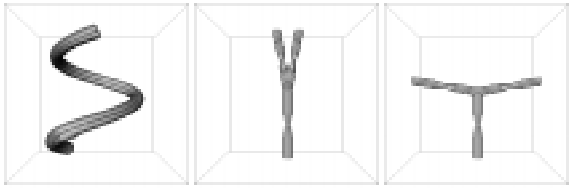

Figure 3 : (from left to right) 3D rendering of a Lissajoux shape, 20° Y fork shape and 160° Y fork shape. Diameter is 4 voxels.

3.1. Tracking of a single structure

On each image, the minimum, maximum and average value of ΔP and $\Delta\Theta$ are measured. Average and standard deviation of those values on the 24 images are listed below in table 1.

	ΔP(mm)		**$\Delta\Theta$ (°)**	
	Avg	Std dev	avg	std dev
Min	0.12	0.01	0.01	0
Max	1.49	0.12	26.32	6.58
Avg	**0.68**	**0**	**1.31**	**0.10**

Table 1 : global results for the tracking of straight tubes and lissajoux shapes.

3.2. Robustness to user interaction

Initial values D_0 and P_0 are interactively provided by the user. The assumptions made on the choice of P_0 and D_0 are that P_0 is inside the vessel to identify, P_0 is not located on a junction, and that the angle between the true orientation of the vessel and D_0 is less than 45°. The limits of the tracking accuracy with respect to the interactive initial values are evaluated :

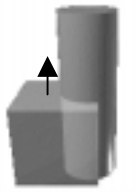

	ΔP(mm)	$\Delta\Theta$ (°)
min	0.01	0
max	2.29	95.93
avg	**0.69**	**2.81**

Initial position outside the structure with good orientation

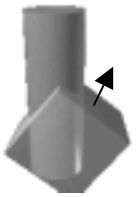

	ΔP(mm)	$\Delta\Theta$ (°)
min	0.11	0.01
max	0.98	44.97
avg	**0.68**	**1.56**

Initial position in the structure - orientation shift : 45°

Table 2 : ΔP and $\Delta\Theta$ values for different initial settings of P_0 and D_0

The tracking fails for orientation shifts superior to 85°. An end of structure is detected instead.

3.3. Application to real images

The vessels in real angiographic images don't exhibit such an ideal grey leve profile. Images are noisy and vessels sometimes present discontinuities or a varying intensity, especially in MRA [3]. The robustness of the tracking method is evaluated relatively to both phenomenons.

The synthetic image of a straight structure is modified as follows (on Fig. 4 from left to right) : two consecutives slices are removed from the image perpendicularly to the structure, the intensity is progressively reduced to 50 % of its original value, and another slice is removed from the image.

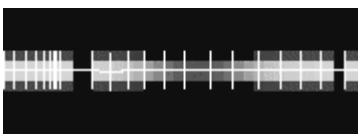

Figure 4 : tracking of a discontinuous structure

	ΔP(mm)	$\Delta\Theta$ (°)
min	0.66	0.01
max	1.44	17.55
Avg	**0.74**	**2.01**

Table 3 : values of ΔP and $\Delta\Theta$ for the tracking of a discontinuous tubular structure

An additive uniform noise is added to the image. The noise level is defined by its amplitude relatively to the maximum intensity in the image.

Noise amp	avg ΔP (mm)	Avg $\Delta\Theta$ (°)
5%	0.68	1.49
10 %	0.69	1.46
20 %	0.73	5.02

Table 4 : average values of ΔP and $\Delta\Theta$ at different levels of noise.

The tracking method fails when the noise value reaches the intensity of the structure to be detected. Voxels belonging to the background become connected to the structure.

We estimate the expected error on cross-sectional area measurement as $err = 1\text{-}\cos^2(\Delta\Theta)$. *err* is always inferior to 1 %. Significant results for further quantitative measurements were obtained.

3.4. Evaluation of the junction detection

Junctions from 20° to 160° are always detected by our algorithm. Failure occurs for angles of 10° or less and 170° or more. Figure 5 shows the tracking of a complex structure with 3 bifurcations ranging from 20° to 70°.

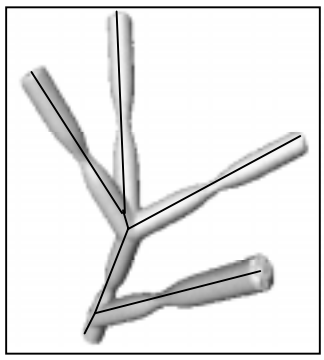

Figure 5 : tracking of a complex structure

4. RESULTS ON ANGIOGRAPHIC IMAGES

4.1. Image pre-processing

The method is applied to 3D Magnetic Resonance Angiograpy (MRA) images of the cerebral vascular network. A specific imaging sequence is designed and the resulting image is segmented before tracking [2].

We show results of our tracking algorithm on MRA and Digital Substracted Angiography (DSA) image. As the vessels present a strong contrast in DSA images, a simple thresholding is used as pre-processing.

4.2. Results on MRA images

No reference centerline is available to assess the quality of our tracking algorithm. Results are visually examined. Vascular tree is well detected. Centerlines are well located for carotid arteries, middle cerebral arteries and the vertebral artery (Fig. 6).

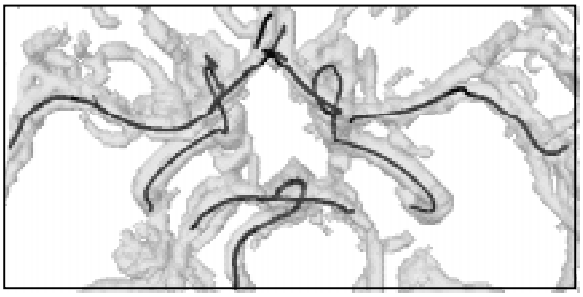

Figure 6 : part of the tracking of the cerebral arterial tree from 3 seed points.

The tracking process doesn't stop at the stenosis location, and the detected centerline follows the axis of the vessel (Fig. 7).

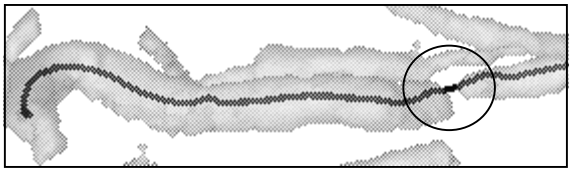

Figure 7 : carotid artery stenosis tracking

4.3. Results on DSA image

DSA is another imaging modality for blood vessels. The substraction between two acquisition steps provides an improved contrast on the resulting image. The image is located at the top of the inferior members (femoral artery).

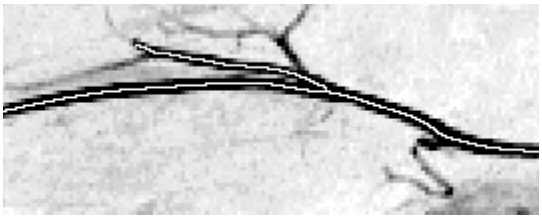

Figure 8 : A part of the tracking process on a DSA image of the inferior members.

5. CONCLUSION

In this paper, tracking of tubular objects network from 3D images has been presented and tested on synthetic images. The proposed method is a full 3D one and handles a large range of bifurcations. Its accuracy is better than 0.4 mm in position and 6° in orientation on synthetic images. The algorithm shows robustness to user interaction, noise and discontinuities in the structures.

The method is applied to MRA healthy volunteers and pathologic images after image pre-processing. The tracking algorithm has also been succesfully tested on Digital Substracted Angiograms (DSA) of inferior members area. Current works focus on 2D and 3D quantification of vessel diameter and cross-sectionnal area to help visualization and stenosis detection.

6. REFERENCES

[1] Farin G., *Courbes et Surfaces pour la GCAO*, Masson, Paris, 1992

[2] Flasque N., Desvignes M., Constans J.M., Revenu M., "Tubular objects network detection from 3D images", 4th Southwest Symposium on Image Analysis and Interpretation proceedings, Austin, TX, pp 96-100, 2000

[3] Hoogeveen R., Bakker C., Viergever M., "Limits to the accuracy of Vessel Diameter Measurement in MR Angiography", JMRI 8 (6), pp 1228-1239, 1998

[4] Krissian K.,. Malandain G., Ayache N., Vaillant R.and Trousset Y. "Model based Multiscale Detection of 3D vessels", IEEE Computer Vision and Pattern Recognition, pp 78-82., 1998

[5] Verdonck B. *Blood vessel segmentation, quantification and visualization for 3D MR and spiral CT angiography*, Ph.D thesis, ENST, Paris, 1996

[6] Wilson D.L., Noble J.A.,"An Adaptative Segmentation Algorithm for Time-of-flight MRA Data", IEEE Transactions on Medical Imaging, 18(10), pp 932-945, 1999